Brief Communication

MOLECULAR METABOLISM

Glycerol not lactate is the major net carbon source for gluconeogenesis in mice during both short and prolonged fasting

Yujue Wang [1], Hyokjoon Kwon [1], Xiaoyang Su [1,2], Fredric E. Wondisford [1,2,*]

ABSTRACT

Objective: Fasting results in major metabolic changes including a switch from glycogenolysis to gluconeogenesis to maintain glucose homeostasis. However, the relationship between the length of fasting and the relative contribution of gluconeogenic substrates remains unclear. We investigated the relative contribution of glycogen, lactate, and glycerol in glucose production of male C57BL/6 J-albino mice after 6, 12, and 18 h of fasting.

Methods: We used non-perturbative infusions of $^{13}C_3$ lactate, $^{13}C_3$ glycerol, and $^{13}C_6$ glucose combined with liquid chromatography mass spectrometry and metabolic flux analysis to study the contribution of substrates in gluconeogenesis (GNG).

Results: During infusion studies, both lactate and glycerol significantly label about 60% and 30–50% glucose carbon, respectively, but glucose labels much more lactate (~90%) than glycerol carbon (~10%). Our analyses indicate that lactate, but not glycerol is largely recycled during all fasting periods such that lactate is the largest direct contributor to GNG via the Cori cycle but a minor source of new glucose carbon (overall contribution). In contrast, glycerol is not only a significant direct contributor to GNG but also the largest overall contributor to GNG regardless of fasting length. Prolonged fasting decreases both the whole body turnover rate of glucose and lactate but increases that of glycerol, indicating that the usage of glycerol in GNG become more significant with longer fasting.

Conclusion: Collectively, these findings suggest that glycerol is the dominant overall contributor of net glucose carbon in GNG during both short and prolonged fasting.

Keywords Fasting; Glycerol; Substrate contribution; Gluconeogenesis; Metabolic flux analysis

1. INTRODUCTION

Elevated fasting glucose is commonly used to diagnose diabetes mellitus (DM) [1], and enhanced hepatic glucose production is the major cause of fasting hyperglycemia in DM [2–5]. At an early stage of fasting, glycogen is the major carbon source of glucose; yet as fasting persists, the major carbon source for glucose switches to gluconeogenesis (GNG) which produces glucose from small metabolites such as lactate, glycerol and amino acids [5–7]. The relationship between the length of fasting and the relative contribution of different substrates in GNG, however, remains unclear.

It is believed that lactate is the major substrate contributing to GNG through a process commonly known as the Cori cycle. The dominant role of lactate in GNG is evidenced by experiments showing that enrichment of circulating glucose at steady state is more than half of the enrichment of a circulating lactate tracer [8–11]. However, this conclusion is confounded by the fact that lactate is largely generated from glucose and resynthesized to glucose via the Cori cycle, making lactate the largest direct contributor to glucose carbon but not necessarily a good source for new carbon entering GNG, which we refer to as an overall contribution. However, GNG substrates such as glycerol and amino acids are much less recyclable from glucose during fasting [12,13], making them better candidates to increase overall net contribution of glucose carbon during GNG. Several studies have emphasized the critical roles of glycerol and amino acids in increased GNG found in patients with DM [5,14–16]. Therefore, a better understanding of substrate usage in GNG during normal fasting is necessary.

In this study, we fasted mice for 6, 12, and 18 h to study the relative contribution of different GNG substrates under different fasting conditions. We show that prolonged fasting clearly shifts the metabolomic profiles of circulating metabolites to one enriched in carboxylic acids without significantly affecting the circulating concentration of important GNG substrates. By performing a comprehensive flux analysis, we demonstrate that lactate is the dominant direct contributor but a minor overall contributor to GNG under all three fasted conditions. Glycerol was the second largest direct contributor and the dominant overall contributor to GNG in all three fasting periods. We also showed that the

[1]Department of Medicine, Rutgers-Robert Wood Johnson Medical School, New Brunswick, NJ, 08901, USA [2]Rutgers Cancer Institute of New Jersey, New Brunswick, NJ, 08901, USA

*Corresponding author. Clinical Academic Building, Room 7316, 125 Paterson Street, New Brunswick, NJ, 08901, USA. E-mail: few11@rwjms.rutgers.edu (F.E. Wondisford).

Received September 14, 2019 • Revision received October 29, 2019 • Accepted November 1, 2019 • Available online 9 November 2019

https://doi.org/10.1016/j.molmet.2019.11.005

GNG flux of lactate decreased while that of glycerol remained stable with prolonged fasting. Together, glycerol is the dominant net carbon source for GNG during short and prolonged fasting.

2. METHODS

2.1. Animals

All mice were maintained on a C57BL/6 J-albino background (Jackson Laboratory; B6(Cg)-Tyr^{c-2J}/J). The glucose homeostasis varies throughout the estrus cycle in female mice [17]. To avoid the variation caused by estrus cycles, only male mice were used in this study. Mice were housed in a pathogen-free barrier facility maintained on a 12-hour light/dark cycle. At 3–4 month of age, mice were catheterized in the right jugular vein [18] and recovered for more than 7 days before experiments. All animal studies were approved by the Institutional Animal Care and Use Committees of Rutgers-Robert Wood Johnson Medical School.

2.2. Tracer infusion studies

Catheterized mice were kept in dark phase with food for at least 6 h before the fasting experiment. All mice were transferred to new cages to fast 0, 6, and 12 h followed by 6 h infusion of tracer without food. For the mouse infusion, a tether and swivel system were used to allow mice free movement in the cage (Instech Laboratories). Water-soluble isotope-labeled metabolites tracers (Cambridge Isotope Laboratories) were prepared as solutions in sterile normal saline and infused via the catheter at a constant rate (0.1 μl/g body weight/min). 200 mM $^{13}C_6$ glucose, 150 mM $^{13}C_3$ glycerol or 40 mM $^{13}C_3$ sodium pyruvate with 360 mM $^{13}C_3$ lactate were prepared as the infusate. The purpose of using a mixture of $^{13}C_3$ sodium pyruvate and lactate is to maintain their physiological ratio (1:9) in the serum. About 30 μl blood were collected by tail vein bleeding after 5 and 6 h of infusion, placed at room temperature in the absence of anticoagulant for 30 min, and centrifuged at 4 °C to prepare serum. At the end of the last tracer infusion experiment, the mice were euthanized by cervical dislocation and quickly dissected liver was snap frozen in liquid nitrogen. Serum and tissue samples were kept at −80 °C until further analysis.

2.3. Glycerol derivatization for LC-MS analysis

Due to the poor ionization of glycerol, an enzymatic derivatization is required to detect glycerol in liquid chromatography mass spectrometry (LC-MS) [19]. Samples containing glycerol were added into 10 × volume of reaction buffer containing 25 mM Tris (pH 8.0), 10 mM Mg^{2+}, 50 mM NaCl, 5 mM ATP, and 2 U/ml glycerol kinase (Sigma-Aldrich) and incubated for 10 min at room temperature. The reaction was quenched with 40:40:20 methanol:acetonitrile:water solution with 0.1% formic acid, and later neutralized with NH_4HCO_3 solution. The same reaction was also performed on blank to remove background. The ion counts of glycerol-3-phosphate in blank was subtracted from that of the derivatized sample.

2.4. LC-MS analysis

Serum samples were mixed with −20 °C 40:40:20 methanol:acetonitrile:water solution with 0.1% formic acid, followed by vortexing for 10 s, incubation at 4 °C for 10 min, and centrifugation at 4 °C and × 16,000 g for 10 min. The volume of the extraction solution was 25 × the volume of serum. The supernatant was transferred to a clean tube, and neutralized with NH_4HCO_3 solution. The mixture was centrifuged again at 4 °C and × 16,000 g for 10 min. The supernatant was then transferred to another clean tube for LC-MS analysis.

LC separation was achieved on a XBridge BEH Amide column (2.1 mm × 150 mm, 2.5 μm particle size, 130 Å pore size; Waters) using a gradient of solvent A (20 mM ammonium acetate + 20 mM ammonium hydroxide in 95:5 water:acetonitrile, pH 9.4) and solvent B (20 mM ammonium acetate + 20 mM ammonium hydroxide in 20:80 water:acetonitrile, pH 9.4). Flow rate was 300 μl min^{-1}. Samples were running using a isocratic method lasting for 6 min, 73% B. The autosampler temperature was set to 4 °C and the injection volume was 5 μL. For a better metabolome coverage, the *m/z* scan range was set to 72–1000 *m/z* at a resolution of 70,000 under negative polarity with AGC target of 3e6 and a maximum IT of 500 ms. Data were analyzed using MAVEN [20]. The isotope natural abundances were corrected using AccuCor [21].

2.5. Liver glycogen measurement

Liver glycogen content were measured using the Glycogen Assay Kit (Sigma-Aldrich).

2.6. Metabolomic analyses

All the heatmaps and principle component analyses were performed on the serum samples after 0, 6 and 12 h fasting followed by 6 h infusion of $^{13}C_6$ glucose. The graphs were generated using R and GraphPad Prism software.

2.7. Metabolic flux analyses

2.7.1. F_{circ} calulation

The calculation of F_{circ} (turnover rate of metabolites) is based on the labeled fraction of tracers and the infusion rate at steady state using the following equation:

$$F_{circ} = Infusion\ rate * \left(\frac{1}{labeled\ fraction\ of\ tracer} - 1 \right) \quad (1)$$

2.7.2. Flux modeling

The relative contributions from substrates are calculated by an elementary metabolite units (EMU) based method [22]. In brief, a flux network is constructed (Supplementary Fig. 1a; Supplementary Table 1; Supplementary Fig. 2). All fluxes were calculated in the unit of nmol product/g/min. All fluxes occur in the liver except V_{out}, V_{glc}, V_3, V_5, V_6, and V_9, which occur in the periphery. V_2, V_5, V_9, V_{13}, and V_{19} are input fluxes from glycogen, glycerol (from triglycerides), lactate (including alanine and pyruvate), free fatty acid (FFA), and amino acids (via TCA cycle) respectively. V_{glc} represents the infusion flux from $^{13}C_6$ glucose tracer. V_{11} is pyruvate carboxylase flux that incorporates carbon dioxide. V_{10}, V_{12}, V_{17}, and V_{18} are decarboxylase fluxes that release carbon dioxide. V_{flop} is an infinitely large flux to account for the symmetry of succinate. V_3 represents the glycolysis process in peripheral tissue. V_6 represents glycerol synthesis from glucose. V_1 is the endogenous glucose production (EGP) flux which equals to the sum of the glucose recycled via the Cori cycle (V_3), glycerol synthesis (V_6), and the net production of glucose (V_{out}–V_{glc}). Therefore, the absolute value of V_1 can be measured as the steady-state glucose turnover rate (F_{circ}) in circulation.

The contribution of amino acids through TCA cycle consists of three components: 1. via oxaloacetate (Asp, Asn); 2. via fumarate or succinyl CoA (Phe, Tyr, Ile, Met, Val, Thr); 3. via α-ketoglutarate (Gln, Glu, Pro, His, Arg). The average physiological concentrations of amino acids are

13.5 μM Asp, 35.9 μM Asn, 54.1 μM Phe, 46.7 μM Tyr, 73.1 μM Ile, 52.4 μM Met, 178.7 μM Val, 126.2 μM Th, 25.1 μM Glu, 397.0 μM Gln, 67.4 μM Pro, 49.6 μM His, and 93.4 μM Arg [23]. Therefore, the total substrate concentration in the three possible pathways are 49.4, 531.2, and 632.5 μM, respectively. Assuming proportional contribution by the three routes, the three sub-fluxes to oxaloacetate, succinate and α-ketoglutarate are 4%, 44%, and 52% of V_{19}, respectively.
The metabolite mass balance leads to the following equations:

$$\text{Glucose: } V_1 - 0.5V_3 - 0.5V_6 + V_{glc} = V_{out}$$

$$\text{G6P: } V_1 - V_4 = V_2$$

$$\text{DHAP: } 2V_4 - V_7 = V_8$$

$$\text{Glycerol: } V_8 - V_6 = V_5$$

$$\text{PEP: } V_7 - V_{10} = 0$$

$$\text{Pyr: } V_{11} + V_{12} - V_3 = V_9$$

$$\text{Oxa: } V_{10} + V_{15} + V_{16} - V_{11} - V_{14} = 0.04V_{19}$$

$$\text{Ac-CoA: } V_{16} - V_{12} = V_{13}$$

$$\text{Suc: } V_{14} - V_{15} - V_{17} = 0.44V_{19}$$

$$\text{Cit: } V_{16} - V_{18} = 0$$

$$\text{aKG: } V_{17} - V_{18} = 0.52V_{19} \quad (2)$$

Balance of input and output mass leads to the following equation:

$$6V_{out} = 6V_2 + 6V_{glc} + 3V_5 + 3V_9 + 2V_{13} + 4.52V_{19} - V_{12} - V_{10} - V_{17} - V_{18} + V_{11} \quad (3)$$

Nine fluxes are designated free fluxes: V_2, V_3, V_5, V_9, V_{12}, V_{13}, V_{15}, V_{19}, and V_{glc}. All other fluxes can be expressed using the free fluxes or known constants ([Eq. (4)]).

$$V_1 = EGP = F_{circ}$$

$$V_4 = F_{circ} - V_2$$

$$V_6 = 2F_{circ} - 2V_2 - V_3 - V_5 - V_9 + V_{12} - V_{19}$$

$$V_7 = V_3 + V_9 - V_{12} + V_{19}$$

$$V_8 = 2F_{circ} - 2V_2 - V_3 - V_9 + V_{12} - V_{19}$$

$$V_{10} = V_3 + V_9 - V_{12} + V_{19}$$

$$V_{11} = V_3 + V_9 - V_{12}$$

$$V_{14} = V_{12} + V_{13} + V_{15} + 0.96V_{19}$$

$$V_{16} = V_{12} + V_{13}$$

$$V_{17} = V_{12} + V_{13} + 0.52V_{19}$$

$$V_{18} = V_{12} + V_{13}$$

$$V_{out} = 0.5*(V_5 + V_9 + V_{19} - V_{12}) + V_2 + V_{glc}$$

$$V_{flop} = \text{Infinite} \quad (4)$$

Since the labeling patterns of all the input molecules are known (either unlabeled or fully labeled as tracer), the steady-state labeling patterns of all metabolites in the system can be calculated using the EMU approach given any set of the nine fluxes. The calculated labeling patterns were compared to the measured ones with equal weight. The best estimated flux set is obtained by minimizing the sum of squared residues (SSR) between the calculated and measured labeling patterns. The measured labeling patterns of glucose, glycerol and pyruvate under three tracers ($^{13}C_3$ glycerol, $^{13}C_3$ lactate, and $^{13}C_6$ glucose) were used in this process. The numerical simulation of labeling patterns was achieved in R software and the optimization was achieved with DEoptim package [24]. 95% confidence intervals were calculated by (1) move one target flux away from the best-fit value by a small step (2) choosing a combination of the other fluxes that minimize the increase of SSR, (3) calculate the new SSR and repeat step (1) to (3) until the new SSR reached the cutoff for 95% confidence interval [25]. The goodness of fit was tested by chi-square test, $X^2_{0.05}$ (df = 15) = 24.996, which is equivalent to a SSR value of 0.0024996. The 15 degrees of freedom are based on 24 measurements (labeling fractions of three metabolites under three tracers) and having 9 unknown fluxes; 24−9 = 15.

2.7.3. Five-pool network

To illustrate the direct and overall contribution better, we simplified the pathways into the 5-pool network (Supplementary Fig. 1b). For convenience, all units of fluxes were normalized to nmol C/g/min. U_1 and U_2 are input fluxes from glycerol and lactate respectively. U_5 and U_6 represent fluxes that glucose making the glycerol and lactate respectively. U_7, U_8, U_3 and U_4 represents the fluxes that glycerol, lactate, glycogen, and TCA amino acids making glucose respectively. U_9 represents the pyruvate dehydrogenase (PDH) flux that consumes lactate in TCA cycle. U_{out} is the glucose output which equals to the net production of glucose. By definition, all fluxes can be represented by the equivalent fluxes in the EMU model:

$$U_1 = 3V_5;\ U_2 = 3V_9;\ U_3 = 6V_2;\ U_4 = 3V_{19};\ U_5 = 3V_6;$$

$$U_6 = 3V_3;\ U_7 = 3V_8;\ U_8 = 3V_{11};\ U_9 = 3V_{12};\ U_{out} = 6(V_{out} - V_{glc}) \quad (5)$$

The direct contribution from glycerol, lactate, glycogen, and TCA amino acids are calculated as the relative ratio of U_7, U_8, U_3, and U_4 respectively (green arrow; Supplementary Fig. 1b). The overall contribution from glycerol, lactate, glycogen and TCA amino acids are calculated as the relative ratio of U_1, U_2, U_3, and U_4 respectively (purple arrow; Supplementary Fig. 1b).

2.7.4. Substrate specific flux calculation

The substrate specific flux of gluconeogenesis is calculated by multiplying the overall contribution to glucose by the glucose F_{circ} measured from the $^{13}C_6$ glucose infusion experiment.

2.8. Statistical analyses

Statistical analyses were performed using the GraphPad Prism software, version 7.04.

3. RESULTS

3.1. Prolonged fasting increases serum carboxylic acid levels but has little effect on GNG substrates

To investigate the effects of fasting on concentrations of serum metabolites, we generated the serum metabolomic profiles of mice after 6, 12, or 18 h of fasting (Figure 1a). In general, the serum profiles of 12 and 18 h fasted mice were similar, while the serum profile from 6 h fasted mice was clearly different. Consistent with these findings, the principle component analysis (PCA) showed a significant separation of samples prepared from the three fasting conditions with 12 and 18 h samples appearing closer to each other and separated from 6 h samples (Figure 1b). We then identified all serum metabolites that showed significantly different concentrations in 6 and 18 h fasted mice and found the majority of the metabolites increased after 18 h of fasting are carboxylic acids (red; Figure 1c, Supplementary Table 2). Glucose and pantothenate/vitamin B_5, a precursor for coenzyme A, are the only metabolites found to be significantly decreased after 18 h of fasting. Interestingly, none of the GNG substrates including pyruvate, lactate, glycerol, and amino acids showed significant changes between the 6 and 18 h of fasting (green; Figure 1c, Supplementary Table 2), suggesting prolonged fasting has little impact on the pool size of GNG substrates.

3.2. Prolonged fasting increases glycerol turnover but decreases lactate and glucose turnover

To investigate the kinetics of GNG substrates during short and prolonged fasting, we fasted mice as described above and infused one of three tracers ($^{13}C_3$ lactate, $^{13}C_3$ glycerol, or $^{13}C_6$ glucose) for 6 h before blood sampling (Figure 2a), which is sufficient to achieve isotopic steady states for all three tracers [26] (Supplementary Figs. 3a and 3b). No significant difference of glucose or insulin level was found across different tracer usage (Supplementary Figs. 3c and 3d), suggesting similar physiological conditions under different tracers. We then calculated the average carbon enrichment (Figure 2b–d). When we infused $^{13}C_6$ glucose or $^{13}C_3$ lactate, enrichment in lactate or glucose was enhanced, respectively, without significant enrichment in glycerol, suggesting that glucose and lactate are interconvertible (Figure 2b, c). In contrast, when we infused $^{13}C_3$ glycerol, both glucose and lactate showed substantial enrichment (30–50% of the $^{13}C_3$ glycerol tracer), indicating that glycerol is converted to both glucose and lactate efficiently (Figure 2d) but little glucose is converted to glycerol (Figure 2b).

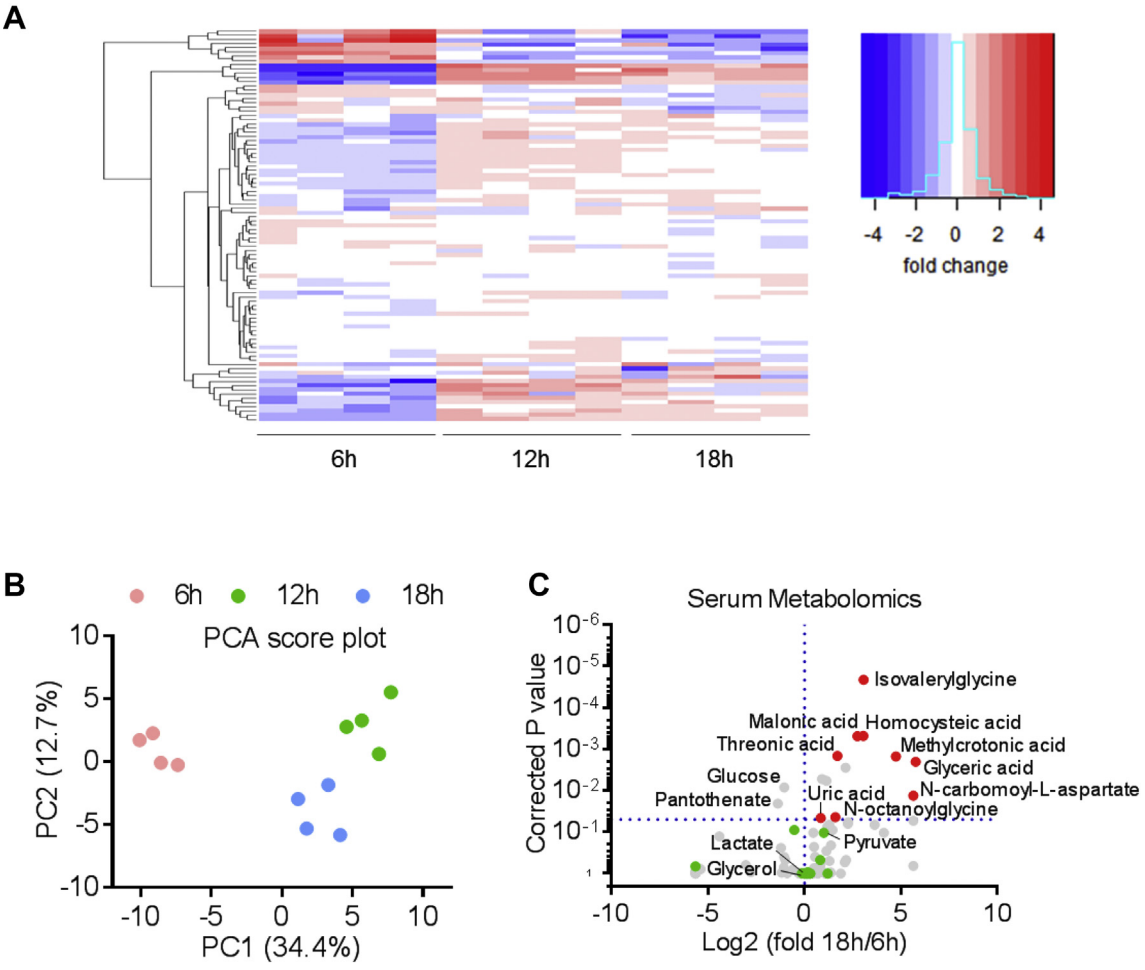

Figure 1: Metabolomic profiles after short and prolonged fasting. A, Heatmap of serum metabolite clusters. Each column represents one mouse and each row represents one metabolites. **B,** Principle component analysis (PCA) of metabolomic profile. Each dot represents one mouse. PC1 and PC2 are the two component explained the highest variance. **C,** Volcano plot of serum metabolomic fold changes between mice fasted for 6 and 18 h. Each dot represents a metabolite: red, carboxylic acids with significant changes; green, gluconeogenic substrates. P values were calculated using two-sided Student's *t*-test and corrected for multiple comparisons using the Holm-Sidak method. $P < 0.05$ is considered significant. $n = 4$ mice for each group. See also Supplementary Table 1.

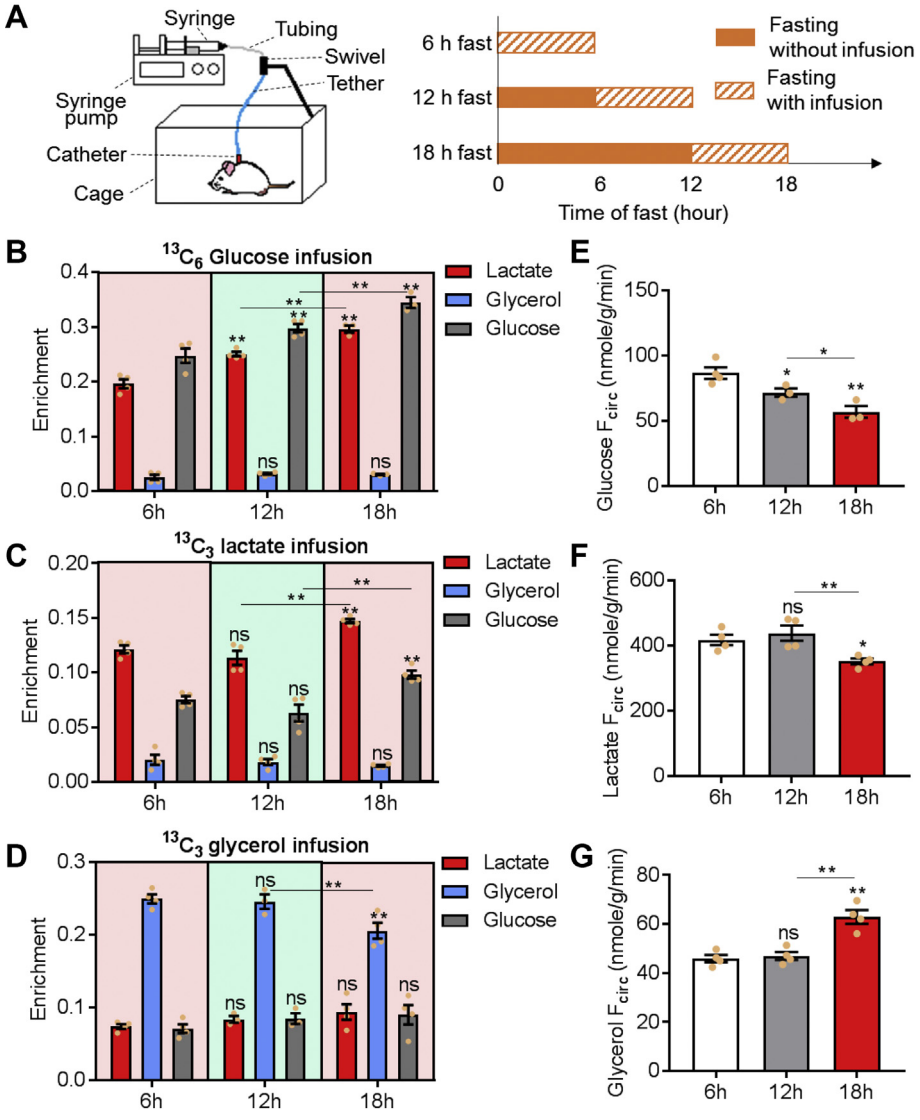

Figure 2: Prolonged fasting increases glycerol turnover and decreases lactate and glucose turnover. A, Experimental scheme of ^{13}C tracer infusions. **B-D,** ^{13}C average carbon enrichment of serum metabolites at steady state infused with $^{13}C_6$ glucose, $^{13}C_3$ lactate, or $^{13}C_3$ glycerol tracers. **E-G,** Turnover rate (F_{circ}) of circulating glucose, lactate, and glycerol. For all experiments, n = 3 or 4 for each group. All data are expressed as mean ± s.e.m. $^{**}P < 0.01$; $^{*}P < 0.05$; ns = not significant by one-way ANOVA. All comparisons are against 6 h data unless indicated otherwise.

Next, we calculated endogenous turnover rates (F_{circ}, Figure 2e–g) of circulating glucose, lactate and glycerol. The turnover rate of glucose continuously decreased from 6 to 18 h (Figure 2e), suggesting a decrease in total glucose production with prolonged fasting. In contrast, lactate and glycerol exhibit no significant changes between 6 and 12 h of fasting, but showed a significant decrease and increase, respectively at 18 h of fasting (Figure 2f, g).

3.3. Glycerol is less recyclable glucose precursor than lactate

Because only one tracer was used at a time and that tracer was the only ^{13}C source in all of the three ^{13}C tracer infusion studies, the relative contribution from the tracer to other metabolites can be estimated using the following equation:

$$\text{Relative contribution} = \frac{\text{Enrichment of metabolite}}{\text{Enrichment of tracer}} \quad (6)$$

For example, in the $^{13}C_3$ lactate infusion, the relative contribution of glucose from lactate can be estimated by the enrichment ratio of glucose versus lactate. Using this method, we compared the interconversion between lactate and glucose (Figure 3a) and between glycerol and glucose (Figure 3b). In all three fasting conditions, lactate contributed about 60% of glucose carbon while glucose contributed about 90% of lactate carbon (Figure 3a). In addition, the fraction of glucose from lactate are significantly lower than the fraction of lactate from glucose in all three fasting conditions. In contrast, glycerol contribution to glucose increased from 30% to 50% with prolonged fasting while glucose contribution to glycerol remained at about 10% (Figure 3b). In all three fasting conditions, the fraction of glucose from glycerol are significantly higher than the fraction of glycerol from glucose. Overall, these data suggest that glycerol is a much less recyclable glucose precursor than lactate under fasting conditions

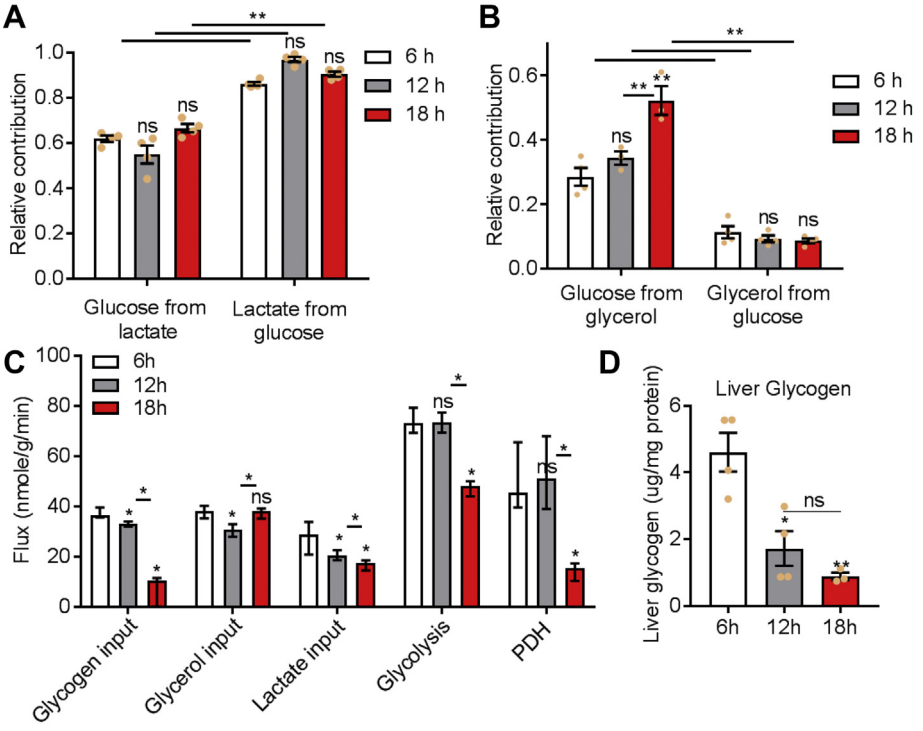

Figure 3: Estimate fluxes in glucose GNG. A-B, Relative contribution of gluconeogenic substrate and product represented by the ratio of ^{13}C enrichment (metabolite versus tracer). **C,** Estimated fluxes in gluconeogenesis pathway. **D,** Liver glycogen content. Data are mean ± s.e.m in **A, B** and **D** and best-fit value ± 95% confidence interval in **C**. n = 3 to 4 mice in each group, **P < 0.01; *P < 0.05; ns = not significant by one-way ANOVA. All comparisons are against 6 h data unless indicated otherwise. PDH, pyruvate dehydrogenase; See also Supplementary Fig. 1 and Supplementary Fig. 3.

since about 90% of lactate is recycled from glucose while only 10% of glycerol is recycled from glucose.

3.4. Prolonged fasting has significant impacts on gluconeogenic fluxes

The enrichment ratio method is only a rough estimation of the relative contribution because it assumes all non-tracer metabolites are unlabeled and therefore overestimates contributions from the tracer. To accurately evaluate the relative contribution from different substrates, we developed a mathematical model that enumerates different flux combinations and simulates the labeling pattern of metabolites associated with each combination (Supplementary Fig. 4). The best-fit flux is the one associated with the least residue between simulated and observed labeling patterns. Using this method, we are able to estimate all the essential fluxes in GNG pathway (Figure 3c; Supplementary Fig. 1a). The input fluxes of glycogen and lactate showed continuous and significant decreases with prolonged fasting. In contrast, the input flux of glycerol remained relatively stable between 6 and 18 h. The fluxes of glycolysis and PDH also decreased from 12 to 18 h. Interestingly, the change of the glycogen flux over time is not in the same pattern as the liver glycogen content (Figure 3d). For example, between 6 and 12 h fasting, the liver glycogen content was reduced by 63% while the glycogen flux was only reduced by 10%. Our analyses have also tested the possibility of a pathway that directly convert glycerol to lactate/pyruvate without passing through glucose (Supplementary Fig. 5). However, in all three fasting conditions, the 95% confidence interval of this flux included 0, suggesting whether this pathway exist or not is inconclusive.

3.5. Lactate is the major direct contributor while glycerol is the major overall contributor to GNG

To illustrate the contribution of substrates better, we summarized all the fluxes into a 5-pool network (Figure 4a–c, Supplementary Table 3) and calculated the direct and overall contribution from all substrates (Figure 4d, e). The direct contribution is the relative ratio of the four fluxes directly making glucose (green arrows, Figure 4a–c) while the overall contribution is the relative ratio of the four overall input fluxes (purple arrows, Figure 4a–c). In all three fasting conditions, lactate exhibits the highest direct contribution to GNG (non-glycogen glucose production) (Figure 4d). However, such a high direct contribution is largely due to the recyclable property of lactate because in terms of the overall contribution, the majority of GNG carbon is ultimately from glycerol (Figure 4e). Interestingly, when glycogen contribution was high (6 and 12 h fast), the contribution from TCA amino acids was negligible. Only when glycogen contribution was diminished at 18 h did the contribution from TCA amino acids start to appear.

Based on the overall contribution data, we next calculated the absolute GNG fluxes specific to each substrate (Figure 4f). Unlike the lactate input flux, which showed continuous decrease with prolonged fasting (Figure 3c), the GNG specific flux from lactate only decreased from 6 to 12 h and remained relatively stable between 12 and 18 h. This is because, between 12 and 18 h, the decrease of PDH flux (Figure 3c) directed more lactate towards glucose rather than acetyl CoA, which overcame the decrease of total lactate input. In contrast, the GNG specific flux from glycerol (Figure 4f) remained relatively stable across different fasting periods. In all three fasting conditions, the gluconeogenic flux from glycerol dominates the other substrates.

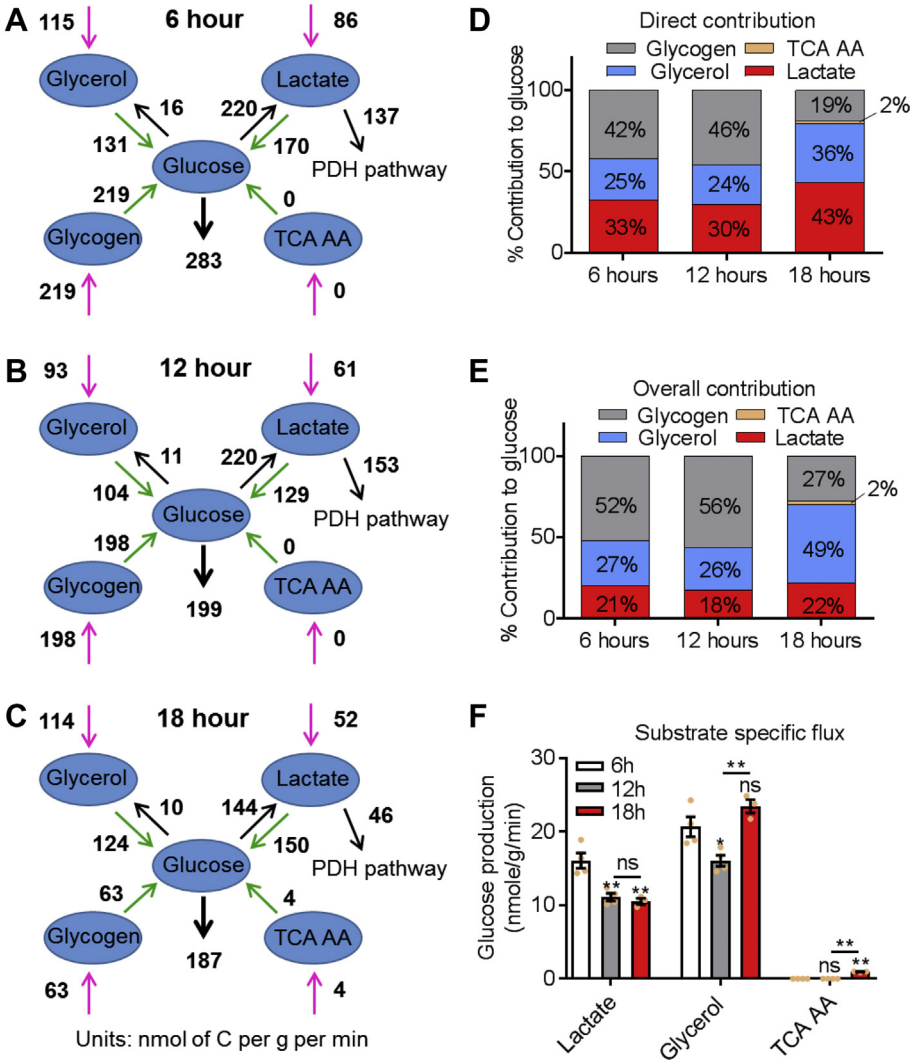

Figure 4: Gluconeogenic contribution. A–C, glucose production network after 6 (**A**), 12 (**B**), and 18 (**C**) hours of fasting. All fluxes are normalized to nmole carbon per gram body weight per minute. The best-fit value are shown for each flux. Fluxes involved in the direct and overall contribution are shown in green and purple respectively. For convenience, all numbers are rounded to the nearest whole number. **D–E,** Direct and overall contribution from lactate, glycerol, glycogen, and TCA amino acids. **F,** Substrate specific gluconeogenic fluxes from lactate, glycerol, and TCA amino acids. Data are mean ± s.e.m.; For all data, n = 3 to 4 mice per group, $^{**}P < 0.01$; $^{*}P < 0.05$; ns = not significant by one-way ANOVA. All comparisons are against 6 h data unless indicated otherwise. PDH, pyruvate dehydrogenase; TCA AA, amino acids that enter gluconeogenesis through TCA intermediates. See also Supplementary Table 3 for confidence intervals of fluxes.

4. DISCUSSION

This study re-evaluated the roles of lactate and glycerol as direct and overall (net carbon) GNG substrate sources during different fasting conditions. Lactate is known as the dominant substrate of GNG based on its high turnover and knowledge that lactate is recycled (Cori cycle). However, the Cori cycle is not a net glucose producer unless lactate is derived from substrates other than existing circulating glucose such as new glucose from glycogenolysis or from GNG substrates such as pyruvate, alanine and glycerol. Consistent with this view, our analysis indicates that although lactate serves as the dominant direct GNG substrate (Figure 4d), its net carbon contribution is too small to account for the total glucose consumption flux. In fact, glycerol through both direct synthesis (Figure 4d) and by labeling a fraction of circulating lactate that subsequently is used in GNG contributes the majority of the net carbon to GNG during all fasting periods (Figure 4e).

Our results demonstrate both the direct and indirect pathway used by glycerol to form glucose based on different labeling patterns of glycerol and lactate-derived glucose (Supplementary Fig. 3). $^{13}C_3$-labeled glycerol makes glucose that is mainly M+3, suggesting that the glycerol carbon backbone is preserved in the newly made glucose (direct glycerol pathway). In contrast, $^{13}C_3$-lactate generates a significant portion of M+1 and M+2 glucose, suggesting extensive carbon shuffling in the TCA cycle of lactate entering at the beginning of the GNG pathway. Thus the major glycerol to glucose pathway is direct and does not involve lactate as an intermediate. However, some of the glucose derived from glycerol has a M+1 pattern, indicating entry as lactate (Supplementary Fig. 3).

Lactate turnover flux during fasting is reported to be more than twice that of glucose [9]. One potential consumer of serum lactate in a fasting animal is the Cori cycle, but, as Hui and colleagues have recently shown, another more important consumer of lactate in most

peripheral tissues except the brain is the TCA cycle [9]. Knowing that much of circulating lactate is completely metabolized in the TCA cycle makes it now unnecessary to assume that it must be regenerated to glucose in the Cori cycle. In fact, our data suggest a large proportion of lactate was consumed in the TCA cycle through PDH pathway instead of entering GNG (Figure 4a–c). Moreover, assuming these flux data are correct, another source of lactate production beyond glycolysis must be present to support the high lactate flux. Given that glycerol tracer labels about 30–50% of circulating lactate, it remains possible that peripheral glycerol metabolism contributes to lactate production.

A review of the tracer enrichment data suggest this pathway may exist (Figure 2b–d). Assuming that the Cori cycle is responsible for generating lactate from glucose and glucose from lactate, then at equilibrium the enrichment fractions of both glucose and lactate should be similar. However, in the $^{13}C_6$-glucose infusion, the lactate enrichment is lower than glucose enrichment, suggesting entry of unlabeled lactate into the cycle in the periphery. In contrast, in the $^{13}C_3$-glycerol infusion, the ^{13}C enrichment gap between glucose and lactate disappeared, suggesting that glycerol contributes to lactate production independently of glucose production. Therefore, we adapted our flux model to include a direct pathway from glycerol to lactate without a glucose intermediate (Supplementary Fig. 5). Due to uncertainty in estimating flux in the new model, we were unable to establish this direct pathway, but the relatively high upper boundary of the 95% confidence interval suggests that it could potentially account for up to 40% of the total glycerol input flux. Uncertainty is mainly due to high recycling of ^{13}C labeling between glucose and lactate, making it difficult to distinguish a direct (glycerol → lactate) versus indirect (glycerol → glucose → lactate) pathway for lactate generation. To solve this issue, a tracer that is non-recyclable between lactate and glucose seems necessary.

Several limitations of this study are noted. First, the contribution from glycogen and TCA amino acids might be overestimated since our model assumes both glycogen and TCA amino acids are non-recyclable from glucose during fasting. However, this limitation is expected to have limited impact on our conclusions since the contribution from glycogen is excluded when calculating the GNG rate and the overall contribution from TCA amino acids is not dominant in all three fasting conditions. Second, our current flux model assumes TCA amino acids contribute to GNG via a universal pool of TCA intermediates, though, in reality, liver and peripheral tissues may functionally use two separate pools. Future studies will investigate the effect of tissue compartmentalization on flux analyses. Third, a relatively high infusion rate of $^{13}C_6$ glucose tracer was used in this study to obtain accurate enrichment values. Consequently, the glucose consumption rate might be increased during $^{13}C_6$ glucose infusion, although no significant difference was found in glucose or insulin levels during fasting comparing to use of the other two tracers (Supplementary Figs. 3c and 3d). Finally, this study is unable to distinguish the contribution from pyruvate, lactate, and alanine due to the high interconversion rate among these three metabolites *in vivo*. Consequently, the lactate flux we referred in this study also included the contribution from other metabolites (including pyruvate and alanine), which enters GNG via lactate.

It should be noted that mice have faster metabolic rates than humans; therefore, it would take a longer time for humans to reach the same fasting state as described in this study [27]. A rough translation can be achieved based on the fact that it takes 36–40 h of fasting in human subjects to deplete liver glycogen storage [28] while it only takes 12–18 h in mice (Figure 3d). Therefore, fasting for 6, 12, and 18 h in mice is roughly 15, 30, and 45 h in humans respectively. Future studies should be necessary to investigate the direct and overall contribution in human subjects and diabetic mouse models at different fasting states.

5. CONCLUSIONS

The direct contribution of substrates to GNG have been determined by several authors, but none have investigated the net carbon contribution of these substrates in GNG [8,10,11,29–31]. Our findings suggest that glycerol is the major net carbon contributor in GNG during both short and prolonged fasting. Elevated glycerol is an important biomarker for the development of hyperglycemia and type 2 DM [32], and patients with type 2 DM also show significantly increased gluconeogenic flux from glycerol [33,34]. Given the importance of glycerol as the dominant ultimate carbon source of gluconeogenesis, the glycerol metabolic pathway is a potentially important therapeutic target in patients with DM.

AUTHOR CONTRIBUTIONS

FEW conceived the experiments, directed the studies and wrote portions of the manuscript; YW constructed the MFA model, analyzed data, and wrote the manuscript; YW and HK designed and performed experiments; XS directed the construction of MFA model; XS and HK revised the manuscript.

ACKNOWLEDGEMENTS

This work was supported by NIH grants R01 DK063349 (to F.E.W) and the Rutgers Metabolomics Core supported, in part, by the Rutgers Cancer Institute of New Jersey (P30CA072720).

APPENDIX A. SUPPLEMENTARY DATA

Supplementary data to this article can be found online at https://doi.org/10.1016/j.molmet.2019.11.005.

CONFLICT OF INTEREST

None declared.

REFERENCES

[1] American Diabetes Association, 2010. Standards of medical care in diabetes—2010. Diabetes Care 33(Suppl 1):S11–S61. Suppl 1.

[2] Hundal, R.S., Krssak, M., Dufour, S., Laurent, D., Lebon, V., Chandramouli, V., et al., 2000. Mechanism by which metformin reduces glucose production in type 2 diabetes. Diabetes 49(12):2063–2069.

[3] Magnusson, I., Rothman, D.L., Katz, L.D., Shulman, R.G., Shulman, G.I., 1992. *Increased rate of gluconeogenesis in type II diabetes mellitus. A ^{13}C nuclear magnetic resonance study*. Journal of Clinical Investigation 90(4):1323–1327.

[4] Petersen, K.F., Price, T.B., Bergeron, R., 2004. Regulation of net hepatic glycogenolysis and gluconeogenesis during exercise: impact of type 1 diabetes. Journal of Clinical Endocrinology & Metabolism 89(9):4656–4664.

[5] Petersen, M.C., Vatner, D.F., Shulman, G.I., 2017. Regulation of hepatic glucose metabolism in health and disease. Nature Reviews Endocrinology 13(10):572–587.

[6] Wajngot, A., Chandramouli, V., Schumann, W.C., Ekberg, K., Jones, P.K., Efendic, S., et al., 2001. Quantitative contributions of gluconeogenesis to glucose production during fasting in type 2 diabetes mellitus. Metabolism 50(1):47–52.

[7] Katz, J., Tayek, J.A., 1998. Gluconeogenesis and the Cori cycle in 12-, 20-, and 40-h-fasted humans. American Journal of Physiology 275(3 Pt 1): E537–E542.
[8] Kida, K., Nishio, T., Yokozawa, T., Nagai, K., Matsuda, H., Nakagawa, H., 1980. The circadian change of gluconeogenesis in the liver in vivo in fed rats. Journal of Biochemistry 88(4):1009–1013.
[9] Hui, S., Ghergurovich, J.M., Morscher, R.J., Jang, C., Teng, X., Lu, W., et al., 2017. Glucose feeds the TCA cycle via circulating lactate. Nature 551(7678): 115–118.
[10] Ross, B.D., Hems, R., Krebs, H.A., 1967. The rate of gluconeogenesis from various precursors in the perfused rat liver. Biochemical Journal 102(3):942–951.
[11] Kaloyianni, M., Freedland, R.A., 1990. Contribution of several amino acids and lactate to gluconeogenesis in hepatocytes isolated from rats fed various diets. Journal of Nutrition 120(1):116–122.
[12] Jensen, M.D., Chandramouli, V., Schumann, W.C., Ekberg, K., Previs, S.F., Gupta, S., et al., 2001. Sources of blood glycerol during fasting. American Journal of Physiology - Endocrinology And Metabolism 281(5):E998–E1004.
[13] Owen, O.E., Reichard Jr., G.A., Patel, M.S., Boden, G., 1979. Energy metabolism in feasting and fasting. Advances in Experimental Medicine & Biology 111:169–188.
[14] Stumvoll, M., Perriello, G., Meyer, C., Gerich, J., 1999. Role of glutamine in human carbohydrate metabolism in kidney and other tissues. Kidney International 55(3):778–792.
[15] Hankard, R.G., Haymond, M.W., Darmaun, D., 1997. Role of glutamine as a glucose precursor in fasting humans. Diabetes 46(10):1535–1541.
[16] Newsholme, P., Brennan, L., Bender, K., 2006. Amino acid metabolism, β-cell function, and diabetes. Diabetes 55(Supplement 2):S39.
[17] Santiago, A.M., Clegg, D.J., Routh, V.H., 2016. Ventromedial hypothalamic glucose sensing and glucose homeostasis vary throughout the estrous cycle. Physiology & Behavior 167:248–254.
[18] Bardelmeijer, H.A., Buckle, T., Ouwehand, M., Beijnen, J.H., Schellens, J.H., van Tellingen, O., 2003. Cannulation of the jugular vein in mice: a method for serial withdrawal of blood samples. Lab Animal 37(3):181–187.
[19] Chiles, E., Wang, Y., Kalemba, K.M., Kwon, H., Wondisford, F.E., Su, X., 2019. Fast LC-MS quantitation of glucose and glycerol via enzymatic derivatization. Analytical Biochemistry 575:40–43.
[20] Clasquin, M.F., Melamud, E., Rabinowitz, J.D., 2002. LC-MS data processing with MAVEN: a metabolomic analysis and visualization engine. In: Current protocols in bioinformatics. John Wiley & Sons, Inc.
[21] Su, X., Lu, W., Rabinowitz, J.D., 2017. Metabolite spectral accuracy on orbitraps. Analytical Chemistry 89(11):5940–5948.
[22] Antoniewicz, M.R., Kelleher, J.K., Stephanopoulos, G., 2007. Elementary metabolite units (EMU): a novel framework for modeling isotopic distributions. Metabolic Engineering 9(1):68–86.
[23] Sugimoto, M., Ikeda, S., Niigata, K., Tomita, M., Sato, H., Soga, T., 2012. MMMDB: mouse multiple tissue metabolome database. Nucleic Acids Research 40:D809–D814. Database issue.
[24] Mullen, K.M., Ardia, D., Gil, D.L., Windover, D., Cline, J., 2011. DEoptim: an R package for global optimization by differential evolution. Journal of Statistical Software 1(Issue 6), 2011.
[25] Antoniewicz, M.R., Kelleher, J.K., Stephanopoulos, G., 2006. Determination of confidence intervals of metabolic fluxes estimated from stable isotope measurements. Metabolic Engineering 8(4):324–337.
[26] Mao, C.S., Bassilian, S., Lim, S.K., Lee, W.-N.P., 2002. Underestimation of gluconeogenesis by the [U-13C6]glucose method: effect of lack of isotope equilibrium. American Journal of Physiology - Endocrinology And Metabolism 282(2):E376–E385.
[27] Agoston, D.V., 2017. How to translate time? The temporal aspect of human and rodent biology. Frontiers in Neurology 8:92.
[28] Rothman, D.L., Magnusson, I., Katz, L.D., Shulman, R.G., Shulman, G.I., 1991. Quantitation of hepatic glycogenolysis and gluconeogenesis in fasting humans with 13C NMR. Science 254(5031):573.
[29] Peroni, O., Large, V., Diraison, F., Beylot, M., 1997. Glucose production and gluconeogenesis in postabsorptive and starved normal and streptozotocin-diabetic rats. Metabolism 46(11):1358–1363.
[30] Perry, R.J., Peng, L., Cline, G.W., Butrico, G.M., Wang, Y., Zhang, X.M., et al., 2017. Non-invasive assessment of hepatic mitochondrial metabolism by positional isotopomer NMR tracer analysis (PINTA). Nature Communications 8(1): 798.
[31] Nunes, P.M., Jones, J.G., 2009. Quantifying endogenous glucose production and contributing source fluxes from a single 2H NMR spectrum. Magnetic Resonance in Medicine 62(3):802–807.
[32] Mahendran, Y., Cederberg, H., Vangipurapu, J., Kangas, A.J., Soininen, P., Kuusisto, J., et al., 2013. Glycerol and fatty acids in serum predict the development of hyperglycemia and type 2 diabetes in Finnish men. Diabetes Care 36(11):3732–3738.
[33] Nurjhan, N., Consoli, A., Gerich, J., 1992. Increased lipolysis and its consequences on gluconeogenesis in non-insulin-dependent diabetes mellitus. Journal of Clinical Investigation 89(1):169–175.
[34] Chung, S.T., Hsia, D.S., Chacko, S.K., Rodriguez, L.M., Haymond, M.W., 2015. Increased gluconeogenesis in youth with newly diagnosed type 2 diabetes. Diabetologia 58(3):596–603.

